ANNUAL REVIEWS

Annual Review of Materials Research

Materials Strategies for Organic Neuromorphic Devices

Aristide Gumyusenge,* Armantas Melianas,* Scott T. Keene, and Alberto Salleo

Department of Materials Science and Engineering, Stanford University, Stanford, California 94305, USA; email: ag47@stanford.edu, armantas.melianas@stanford.edu, asalleo@stanford.edu

Annu. Rev. Mater. Res. 2021. 51:47–71

First published as a Review in Advance on April 13, 2021

The *Annual Review of Materials Research* is online at matsci.annualreviews.org

https://doi.org/10.1146/annurev-matsci-080619-111402

*These authors contributed equally to this article

Keywords

artificial synapses, artificial neural networks, resistive memory, bioelectronics

Abstract

Neuromorphic computing is becoming increasingly prominent as artificial intelligence (AI) facilitates progressively seamless interaction between humans and machines. The conventional von Neumann architecture and complementary metal-oxide-semiconductor transistor scaling are unable to meet the highly demanding computational density and energy efficiency requirements of AI. Neuromorphic computing aims to address these challenges by using brain-like computing architectures and novel synaptic memories that coallocate information storage and computation, thereby enabling low latency at high energy efficiency and high memory density. Though various emerging memory devices have been extensively studied to emulate the functionality of biological synapses, there is currently no material/device system that encompasses both the needed metrics for high-performance neuromorphic computing and the required biocompatibility for potential body-computer integration. In this review, we aim to equip the reader with general design principles and materials requirements for realizing high-performance organic neuromorphic devices. We use instructive examples from recent literature to discuss each requirement, illustrating the challenges as well as future research opportunities. Though organic devices still face many challenges to become major players in neuromorphic computing, mostly due to their lack of compliance with back-end-of-line processes required for integration with digital logic, we propose that their biocompatibility and mechanical conformability give them an advantage for creating adaptive biointerfaces, brain-machine interfaces, and biology-inspired prosthetics.

1. BACKGROUND

Device downscaling has long been the main approach to meeting the increasing demands for high-performance computing in silicon-based technologies. However, this approach is reaching practical limits as the von Neumann computer architecture (in which data are constantly transferred between computing units and memory units) and complementary metal-oxide-semiconductor (CMOS) transistor scaling are unable to meet the increasingly demanding requirements for faster computing and larger memory density that are needed to handle the large data sets processed with artificial intelligence applications. The execution of these tasks with minimal power consumption has sparked a new era of research in computing systems, such as brain-like computing (1). The brain has a large memory capacity and simultaneously executes a multitude of tasks (sensing, image recognition, etc.) with much lower power consumption than conventional electronic systems. In the simplified picture, the brain works through a neural network in which signals are transmitted from neuron to neuron as ion fluxes or electrical spikes (2). To emulate brain functionality in silico, neuromorphic computers have been proposed that use emerging synaptic devices as a new computing approach beyond traditional von Neumann computing and conventional semiconductor devices.

To learn and remember (compute and store data) like the brain does, memristive devices (3) have been thoroughly investigated owing to their ability to respond to electrical signals and maintain different conductance states for a long or short time. Such devices are sought after because, in their simplest geometry (two terminal), they are the closest electronic analog to a biological synapse. One of the most promising approaches is to use arrays of such memory devices to accelerate artificial neural network (ANN) algorithms in hardware. This approach takes advantage of the recent success of ANNs in self-driving automobiles and in performing tasks including natural language and image processing, and financial calculations. In such an array, the conductance of each memory device represents the synaptic weight used in software ANNs. Upon training, the conductance of the conducting material can be modulated via materials-dependent mechanisms: formation of a conductive filament, charge trapping/detrapping, ion migration, or a reversible electrochemical reaction (4–6). This conductance modulation emulates the activity of a biological synapse in which an action or chemical potential induces signal transmission across the synaptic cleft (7).

To date, several demonstrations of memory devices have shown promising performance, including mature technologies such as phase change memory (PCM) and resistive random-access memory (ReRAM) (5, 6, 8). Since their demonstration by IBM nearly six decades ago (9, 10), great progress has been achieved using these devices for neuromorphic computing. Several materials, mostly inorganic, have been shown to (*a*) switch at high speed in response to small potential pulses, thus operating with low power consumption (11); (*b*) learn and remember (6) (i.e., conductance switching and state retention); and (*c*) be scalable to <100-nm dimensions using conventional semiconductor foundry processes, which makes them attractive for commercialization (12). However, from a materials standpoint, PCMs and ReRAMs are not ideal since they suffer from inherently stochastic and asymmetric resistance switching that is detrimental for ANN computing. In addition, scaling to large ANN arrays requires low operating currents and low device-to-device variability, which remain some of the major bottlenecks for these technologies. To date, there is no single material or device that successfully meets the entire set of stringent neuromorphic device metrics (e.g., programming linearity, fast switching, low operating current and voltage, low switching energy, high endurance, small footprint, low device-to-device variability, integration compatibility with digital logic). The need to realize efficient synthetic neural systems has led researchers to look beyond conventional materials and devices and explore novel materials and switching mechanisms for neuromorphic computing.

Organic electronic materials have attracted a great deal of attention after demonstrating some of the resistance switching properties found in inorganic materials. Furthermore, organic materials have shown other features, such as biocompatibility, flexibility, and softness, that make them appealing candidates for bioelectronics (13–15). Like inorganic materials, organic materials have demonstrated synaptic behaviors of various kinds depending on the materials system: filament forming (16–18), charge trapping (19–21), redox active (22–26), and ion migration–based (27, 28) memory devices. Though device demonstrations are being reported at an increasing rate, further innovations in materials design, patterning techniques, and device architectures are still needed to explore the full potential of organic electronic materials for neuromorphic computing. For example, typically reported inorganic neuromorphic devices switch at ~10–100-ns timescales and can be scaled down to the ~10–100-nm dimensions that are needed to realize high-density and efficient synthetic neural systems. Simply put, organic neuromorphic devices are lagging behind their inorganic counterparts in terms of technological maturity. While this brings major challenges, there are also promising research opportunities as it is still unclear whether fundamental advantages that organic neuromorphics may exhibit are sufficient to bridge this technological gap.

In this review, we first highlight the device requirements for high-performance neuromorphic computing and discuss how organic electronic materials compare to their inorganic counterparts. We aim to provide materials and device considerations for readers that are interested in exploring organic electronic materials for neuromorphic devices that can be competitive candidates for inorganic systems. The discussion mainly focuses on organic materials functioning as the (semi)conductive component of neuromorphic devices even though organic materials have been studied in other device components, such as substrates and electrolytes. We focus on design strategies for simultaneously meeting all of the device metrics rather than optimizing any single parameter. Since neuromorphic device operation mechanisms have been discussed elsewhere (5, 6, 29, 30), we limit this discussion to materials considerations for combining high-performance neuromorphic computing with other attractive properties found in organic materials. We end Section 2 by discussing remaining challenges and opportunities for the implementation of organic materials in neuromorphic devices.

In Section 3, we discuss the potential for organic neuromorphic systems to interface directly with biological tissues owing to the biocompatibility and softness of organic materials. The utility of ANNs in healthcare has been demonstrated, with examples including diagnosing skin cancer via melanoma images (31), deciphering sleep disorders from electrophysiological recordings (32), and restoring motor functionality in a paralyzed participant (33). With the advances in neuromorphic devices for efficiently emulating ANNs, we expect that the power costs and form factor necessary to run ANNs will continue to be reduced significantly. This efficiency improvement presents an excellent opportunity for direct integration of ANNs with biomedical devices to form adaptable, bioinspired prosthetics and health-monitoring tools. In particular, the favorable materials properties of organic materials make them ideally suited for seamlessly integrated biotic/abiotic neural networks. We review the current work and remaining challenges for organic materials and devices that impact bioinspired and biointegrated computing.

2. DEVICE AND MATERIALS REQUIREMENTS FOR HIGH-PERFORMANCE ARTIFICIAL NEURAL NETWORK COMPUTING

2.1. Introduction to Artificial Neural Network Accelerators

One approach to designing high-performance ANN accelerators relies on selectively mimicking brain functionality. In biological neural networks, signals are transmitted between neurons

through synapses (**Figure 1*a***). At such junctions, the inputs are either excitatory or inhibitory, altering the strength of the signal transmitted to the postsynaptic neuron. Such adaptive connectivity allows the brain to execute a multitude of tasks in response to sensory activity, to learn, and to remember. To learn, the brain relies on one of its greatest features—its synaptic plasticity. That is, a synapse can adapt based on previous inputs through modulation of the connection strength

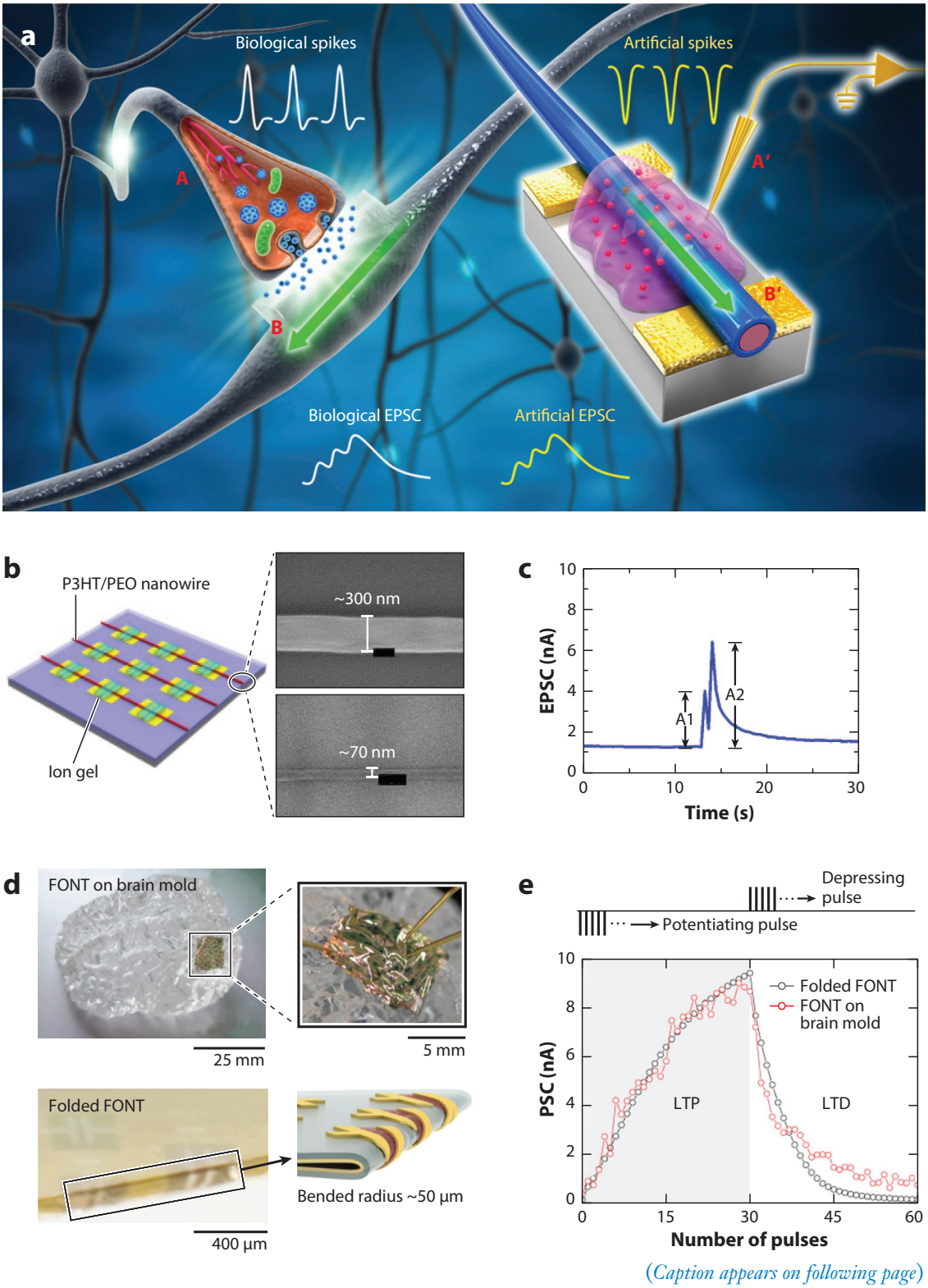

(Caption appears on following page)

Figure 1 (*Figure appears on preceding page*)

(*a*,*b*) Illustration of organic artificial synapses in a SNW-based synaptic transistor using P3HT fibers. The probe (A′) delivers presynaptic spikes to the presynaptic ion gel membrane, which induces mobile ion interaction with the nanofiber (B′), modulating the nanofiber conductance and inducing EPSC. The channel response to presynaptic spikes is then delivered to an artificial postneuron through connections to the drain electrode. Also shown in panel *b* are the scanning electron microscopy images of scaled single fibers down to 70–300 nm in diameter. (*c*) Current responses triggered by two consecutive spikes with an interspike interval of 780 ms. A1 and A2 are the amplitudes of the first and second EPSCs, respectively. Panels *a*–*c* adapted with permission from Reference 41; copyright The Authors, some rights reserved; exclusive licensee American Association for the Advancement of Science (CC BY-NC 4.0). (*d*) Photographs of the conformable FONTs on the brain-shaped PDMS mold and completely folded FONTs. (*e*) Long-term potentiation (500 ms, −30 V) and long-term depression (500 ms, +30 V) of a FONT conforming to the brain-like mold and, when folded, demonstrating the mechanical tolerance of synaptic behavior in organic systems. Panels *d* and *e* adapted with permission from Reference 45; copyright 2019 American Chemical Society. Abbreviations: EPSC, excitatory postsynaptic current; FONT, ferroelectric organic neuromorphic transistor; LTD, long-term depression; LTP, long-term potentiation; P3HT/PEO, poly(3-hexylthiophene-2,5-diyl)/polyethylene oxide; PDMS, polydimethylsiloxane; PSC, postsynaptic current; SNW, single nanowire.

of that synapse, making subsequent signals more or less likely to trigger an action potential. With signal consistency and repeated learning, each synapse becomes capable of adapting to incoming data without supervision to establish a stronger connection (or weaker in case of inhibitory signals) with the adjacent synapse (2, 34, 35).

The power of the brain lies not only in how information is processed at the individual synapse level, but also in the massively parallel way the synapses are wired and communicate with one another. In synthetic neural networks, this adaptive connectivity, though it remains challenging, is emulated using a neuromorphic device that has a variable conductance that represents the synaptic weight. Here, we focus on the device requirements for ANN accelerators, which provide general intuition to the reader interested in neuromorphic computing. We mainly focus on ion-gated synaptic devices due to their excellent performance and similarity to the synaptic cleft in the brain, which also relies on fluxes of chemical species and lies at the cornerstone of describing brain functionality.

In hardware ANNs, an array of neuromorphic devices are needed that (*a*) are programmable in parallel, (*b*) consume minimal energy, (*c*) operate with small currents, (*d*) have predictable and stable switching characteristics, (*e*) can retain the updated state (conductance), (*f*) can effectively update inputs and transmit the outcoming weights onto the next node, and (*g*) execute the above at a high speed. Such an array enables effective feed-forward processes and the execution of summation and multiplication tasks along columns and rows (i.e., in a crossbar) with minimal steps and low energy consumption. In addition to these general characteristics, such synapses should be small enough to realize high density and be readily integrable into existing semiconductor and circuit manufacturing.

2.2. Scaling

To emulate high-performance brain-like computing, the ANN must be made of as many synaptic devices per volume as possible. It is imperative that memory devices are made extremely small and are tightly packed to ensure sufficient memory capacity for hosting the typically large ANN software models in hardware. However, to date, the highest-performing supercomputers remain voluminous and power hungry. In natural organisms, the memory devices (synapses) are only ∼20–40-nm wide and are efficiently packed within the neural network. This length scale is comparable to the memory cell size of no larger than ∼0.1 μm^2, as recently proposed for realizing fast and energy-efficient ANN accelerators (36). As such, when designing and testing any neuromorphic device, it is important to consider the feasibility of ultimately scaling the proposed technology

to ~10–100-nm dimensions. If an efficient neuromorphic device is reported but lacks scalability to submicrometer dimensions and a feasible path for integration into ANNs, such a technology is unlikely to become useful for high-performance computing, while retaining utility in other less-demanding applications. Note that other components of the ANN accelerator circuit, such as the peripheral circuitry driving the artificial synapse arrays, add to the overall hardware volume.

Since memristors can be made in a simple layout, e.g., two-contact architecture, synaptic switching is in principle envisioned to be achievable even at the atomic level in inorganic systems (37–39). The same two-terminal approach has been recently utilized for solution processed organic-metal-complex-based memories, in which device dimensions were controlled by high-resolution sputtering techniques to achieve down to 60-nm^2 two-level memory devices with excellent and robust performance [e.g., fast switching (<30 ns), excellent endurance (~10^{12} cycles), and nonvolatility (over 500 days)] (40). This demonstration shows that memory devices, switching characteristics, and implementation are not inherently limited by size. However, it is yet to be demonstrated whether such two-terminal devices can meet all the needed metrics for high-performance computing utilized in functional ANN arrays and whether such arrays would perform well.

Though organic transistors are commonly large (e.g., several micrometers in channel length), recent efforts using transistor-like architectures have aimed to demonstrate submicrometer organic synaptic devices. For instance, Xu et al. (41) have recently demonstrated that by using polymer nanowires, the size of synaptic devices could be reduced to single nanowire (SNW) transistors. By utilizing poly(3-hexylthiophene-2,5-diyl) (P3HT) coated with polyethylene oxide (PEO), a 70-nm-wide nanofiber could be processed that allowed the researchers to demonstrate a nanowire-based synaptic device with a 300-nm-long channel showing low-energy switching characteristics and learning behaviors (**Figure 1*b*,*c***). With such dimensions, many artificial synapses could potentially be fabricated via printing techniques to form the network needed for ANN accelerators, but this remains to be demonstrated. Note that the device fabrication by Xu et al. (41) involved an on-wire lithography step that is not necessarily compatible with large-scale semiconductor fabrication and back-end-of-line (BEOL) processes, which should be considered for future integration. Nonetheless, the single fiber approach showed not only that organic materials are promising candidates for synaptic devices, but also that with controlled scaling, organic devices could approach the spatial dimensions found in biological systems as well as those suggested by industry experts (36). Future work in this area, exploring novel routes to organic electronic device fabrication at submicrometer dimensions (e.g., using advanced lithography or self-assembly), is of utmost importance to compete with the more mature inorganic technologies.

2.3. Switching Energy and Power Consumption

In biological systems, each synaptic event consumes ~10 fJ of energy that, combined with its massively parallel operation, enables the brain to efficiently execute a multitude of tasks with ~20 W of operating power. For ANN accelerators, the write-erase switching in each synapse (typically 10,000 to 100,000 synapses in an array) should occur at low enough switching energy to achieve the low power of biological computation. To approach the computation efficiency of the brain, the switching energy in artificial synapses needs to be <1 pJ per event (42). As alluded to above, device downscaling is one approach to energy consumption reduction.

The SNW-based P3HT devices demonstrated switching energies as low as 1.23 fJ, rivaling the natural behavior of synapses (41). In thin-film-based devices, van de Burgt et al. (22) demonstrated that poly[3,4-(ethylenedioxy)thiophene]:poly(styrene sulfonate) (PEDOT:PSS) combined with an aqueous electrolyte exhibited a linear scaling of energy consumption with device channel area. These electrochemically switchable devices, sometimes referred to as electrochemical

random-access memory (ECRAM), offered a theoretical energy projection of 35 aJ to switch a 0.3- × 0.3-μm^2 device. Later studies corroborated the low ECRAM energy consumption in solid-state devices using device downscaling and experimentally achieved 80 fJ per write operation in a 15- × 45-μm^2 ECRAM channel (43, 44). Though such area scaling is not unique to organic-based ECRAMs (42), it shows that organic synapses, once scaled to smaller dimensions, can be inherently low power.

2.4. Device Resistance

Since typical hardware ANN crossbar arrays are designed to have ~10,000–100,000 devices per column or row, the current running through each device will eventually add up at the column and row ends during readout. As a result, low-conductance (or low-current) devices are necessary. For example, if each device carries 1 μA of current, 10,000 devices will add up to as much as 10 mA at the row or column end. This will lead to significant Joule heating within the array and possibly electromigration, destroying the metal line. In addition, large currents are symptomatic of large power consumption. Therefore, for ANN accelerators the design rule is to limit the interconnect currents to ~10 μA, or 0.1–1 nA per device (the larger the array, the lower the desired current). Note that ultimately the current at each synapse should remain sufficiently high for sensing at the array periphery.

Such a low current requirement necessitates the use of low-conductance materials, making organic electronic materials particularly attractive candidates since their charge carrier mobilities are inherently low compared to crystalline semiconductors. While for other applications (e.g., solar cells, transistors, sensors) low mobility is a disadvantage, it can be advantageous for neuromorphic computing. More specifically, the low-mobility materials that are typically disregarded following synthesis and initial testing as poor conductors now have an attractive application as low-conductance neuromorphic devices. Furthermore, the conductivity of organic materials can be tuned through molecular design, doping, blending, and even processing. Most organic electronic materials already have an inherently tunable conductance, in comparison to inorganic counterparts, which gives them a competitive edge in this area as long as the materials conductance can be switched efficiently (i.e., while meeting all of the other discussed metrics). For example, in an ECRAM array programmed in parallel (44), it was found that by diluting PEDOT:PSS with an additional PSS insulator within the channel to reduce its conductivity, the quality of the write-read operations could be maintained with low noise and high programming linearity. The diluted channel allowed for the current to be as low as 50 nA using a −0.1-V read voltage. Such low device conductance combined with linear switching is ideal for scaling to large neuromorphic arrays.

Low conductivity synaptic behavior can also be achieved in single material systems. For example, in the case of ferroelectric organic neuromorphic transistors (FONTs), currents as low as 10 nA have been demonstrated by Jang et al. (45). These devices were able to function even when fully folded thanks to their softness, which allowed them to adhere to a brain model having mechanical properties comparable to those of a real brain (**Figure 1*d,e***). However, once the devices are scaled well below the substrate bending radius, their inherent flexibility becomes unimportant as at 100-nm scale the substrate is effectively flat. Having said that, mechanical flexibility is desired for applications in which aggressive device scaling is not needed, e.g., for interfacing with biological systems, as we discuss in Section 3.

2.5. Dynamic Range

Similar to transistors, synaptic devices must also demonstrate distinct high- and low-conductance states. Though the natural brain has evolved to exhibit some neural activity even in response to

chaotic signals, this behavior remains challenging to fully understand and utilize in a synthetic neural system (46). Hardware ANNs thus typically strive for a large and linear dynamic range at each synaptic node to tackle two aspects: device-to-device variation and write noise tolerance. For example, if the device median conductance varies across devices in an array but they have a large dynamic range, all devices in the array can be operated over a common (or smaller) conductance range. This is not possible if the devices have limited and nonoverlapping dynamic ranges.

In principle, while a large dynamic range is desirable, it is not a stringent requirement for neuromorphic computing if the system demonstrates distinct conductance states. In the case of multilevel conductance states, the range must be sufficiently wide to reliably program to all desired states. In other words, a wider dynamic range improves the device tolerance to write noise since with low write noise signals can be better distinguished from environmental perturbations (thermal, mechanical, photo, etc.) as well as inherent device programming noise. Typically, the targeted dynamic range is >330 times larger than the device write noise for high-accuracy ANNs (47). However, there are diminishing returns on increasing the dynamic range beyond a high/low ratio of 10–100× due to the requirement for linear spacing between conductance states. Note that, per the low-conductance requirement, it is best if both the ON and OFF current levels are simultaneously low (e.g., 1–10 Mohm device operation is better than 1–10 kohm operation).

If a device is too sensitive to minute environmental variations, one might consider improving stimulus specificity and sensitivity within the active channel. For instance, Yang et al. (48) recently demonstrated the use of chlorophyll, a light-sensitive and -specific molecule, to achieve light-stimulated synaptic transistors. The transistor devices used a common donor-acceptor diketopyrrolopyrrole-based polymer, but chlorophyll was embedded in the channel, thus affording photo-responsive organic field-effect transistors (49). Owing to high light sensitivity, the resulting synaptic devices could exhibit excellent switching behaviors even when the drain voltage was as low as 10^{-5} V. Such enhancement in stimulus sensitivity is a promising approach for materials candidates that do not inherently exhibit a large dynamic range. However, this approach faces a major challenge in terms of focusing light onto individual devices, especially once the devices are scaled down to the submicrometer dimensions required for practical computing applications.

In more extensively studied transistor devices such as field-effect transistors and ECRAMs, organic semiconductors have already shown sufficiently large dynamic ranges with over 100 states in the linear regime. In addition, several organic systems, such as PEDOT:PSS, P3HT, polyaniline (PANI), and small molecules, can turn from a high-resistance state to a low-resistance state when employed in ReRAMs (50, 51), ECRAMs (22, 52), and FONTs (45). However, a few challenges remain: the ability to switch with linear characteristics and, no less importantly, the ability to exhibit multiple conductance states. To address these challenges, a recent study demonstrated ECRAMs with 4× dynamic range while retaining all of the other neuromorphic device requirements: 20-ns switching, submicrosecond write-read cycling, low noise, and low-voltage (±1 V) and low-energy (~80 fJ per write) operation combined with excellent endurance (>10^9 write-read operations at 90°C), as shown in **Figure 2** (43). This improvement was achieved by utilizing a novel semiconducting polymer, poly(2-(3,3-bis(2-(2-(2-methoxyethoxy)ethoxy)ethoxy)-[2,2-bithiophen]-5-yl)thieno[3,2-b]thiophene) [p(g2T-TT)], which demonstrates one of the hallmarks of organic electronics in tuning synaptic device properties by new materials design.

2.6. Number of Conductance States

When designing ANNs, it is imperative that the functional materials possess distinct states to emulate synaptic behavior. As alluded to above, for hardware ANN accelerators, it is important that each state (e.g., among 100 states) is linearly programmable in response to an external input

(electrical potential or chemical stimulus). For some applications, a two-state device that simply demonstrates high- and low-conductance states can be sufficient, e.g., in low-precision ANN accelerators, but this may hinder overall ANN accuracy. Generally, there is no clear guideline for the number of required conductance states, as this depends on the specifics of the targeted application, particularly the precision of the analog-to-digital conversion (ADC) at the periphery of the array. More concretely, while the ADC performed on the array periphery is typically 8-bit or lower precision and depends on the application, synaptic devices having a high number of and precisely distinguishable states result in higher accuracy even with low-precision ADC. Based on our previous experience, it is reasonable to target analog device operation with 10–100 clearly

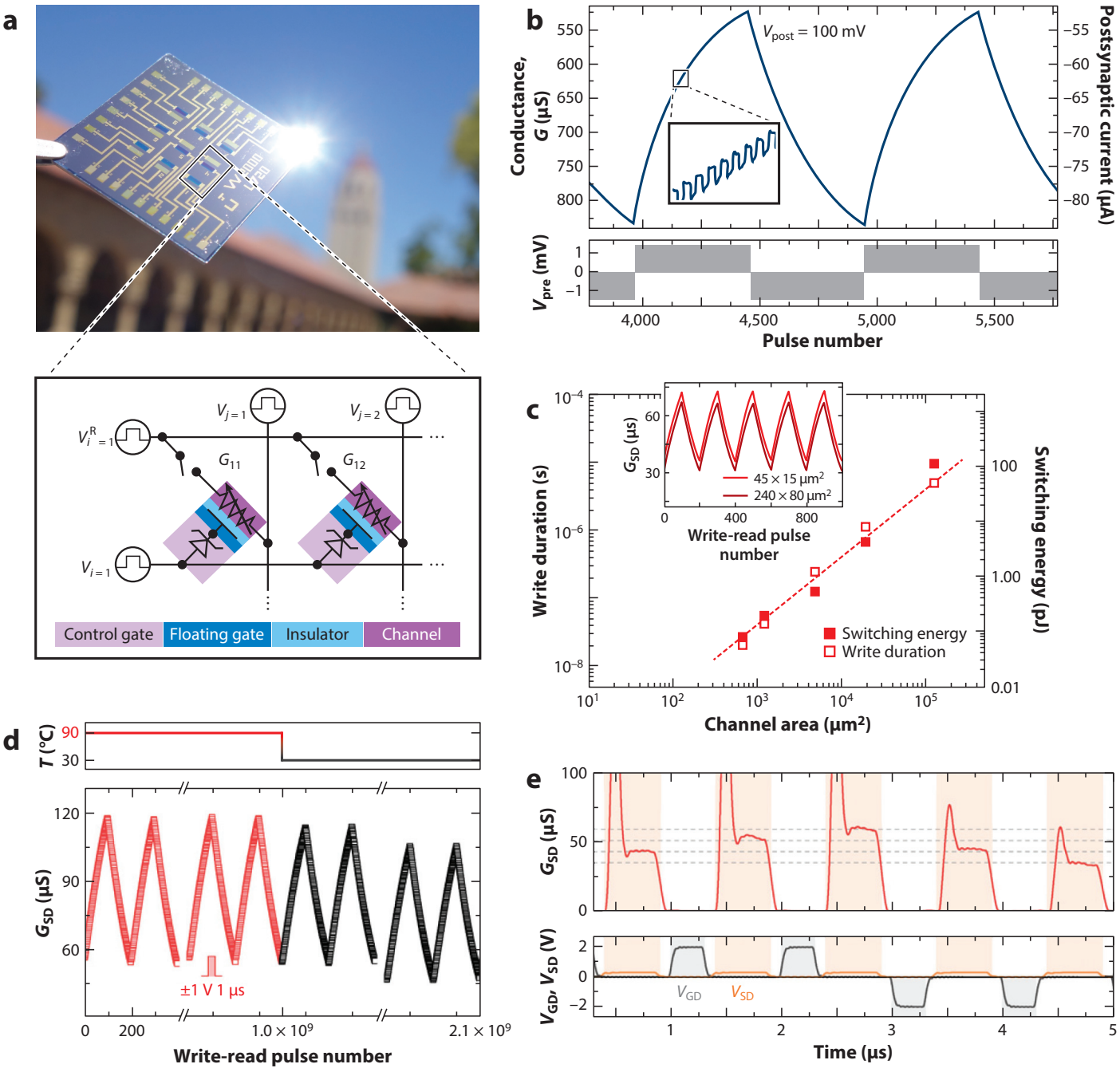

(Caption appears on following page)

Figure 2 (*Figure appears on preceding page*)

Organic artificial synapses for high-performance ANN accelerators. (*a*) Photograph of a 3 × 3 ECRAM prototype before access device integration along with a schematic (1 × 2) of an IFG resistive memory programmable in parallel, which uses a diffusive memristor (control gate) as an access device. The IFG array is programmed by applying voltages V_i and V_j along the rows and columns, respectively. Photo in panel *a* reproduced with permission from A. Melianas and S. Keene; schematic adapted with permission from Reference 44. (*b*) Long-term potentiation and depression displaying 500 discrete states over the operating range in PEDOT:PSS-based ECRAM. The inset is a zoomed-in image showing the individual states. Panel *b* adapted with permission from Reference 22; copyright 2017 Springer Nature. (*c*) Estimated (*dashed line*) and measured (*open* and *closed squares*) redox transistor switching speed and energy scaling with channel area. The inset shows the quality of the switching at selected device dimensions. (*d*) Endurance of ECRAM devices based on p(g2T-TT) to $>10^9$ write-read events at 90°C (*red*), followed by additional $>10^9$ write-read events at 30°C (*black*) using ±1-V, 1-μs pulses. (*e*) Organic ECRAM submicrosecond write-read cycling: potentiation and depression under ±2-V, 200-ns write pulses (*gray shaded area*), followed by 100-ns write-read delay and +0.3-V, 500-ns readout (*orange shaded area*). Panel *c–e* adapted with permission from Reference 43; copyright The Authors, some rights reserved; exclusive licensee American Association for the Advancement of Science (CC BY-NC 4.0). Abbreviations: ANN, artificial neural network; ECRAM, electrochemical random-access memory; GD, gate drain; IFG, ionic floating-gate; p(g2T-TT), poly(2-(3,3-bis(2-(2-(2-methoxyethoxy)ethoxy)ethoxy)-[2,2-bithiophen]-5-yl)thieno[3,2-b]thiophene); PEDOT:PSS, poly[3,4-(ethylenedioxy)thiophene]:poly(styrene sulfonate); SD, source drain.

distinguishable states. For applications that require only short-term plasticity, i.e., a current spike that subsequently decays with time, two-state materials are also suitable.

Write noise is a common problem for conventional resistive switches but has been overcome using ECRAMs (22). For instance, in electrochemically gated devices, PEDOT:PSS exhibited 500 distinct conductance states (**Figure 2*a*,*b***) and extremely low write noise, rendering these states clearly distinguishable (22). Owing to the ability of conjugated polymers to be controllably doped/dedoped upon controlled ion extraction or injection, such multilevel conductance has been less challenging to attain than in inorganic resistive switches (53), e.g., ReRAMs and PCMs, in which the conductance tuning mechanism inherently relies on at least one stochastic process. Modulating conjugated polymer conductivity by ion insertion without degrading the materials is thus quite attractive for realizing synaptic behaviors.

2.7. Quality of Resistive Switching

It is not enough to have resistive switching; the conductance modulation should ideally be linear, symmetric, and low noise for potentiation and depression. In ANN accelerators, a linear response to identical inputs is desired to allow synapses to accurately and repeatably update corresponding weights without knowledge of the initial state. To effectively erase during the learning phase, an opposite and symmetric response is also needed when an opposite stimulus is applied. This is currently a major bottleneck for conventional memristors, such as PCMs and ReRAMs (6). Due to the stochastic nature of the switching behavior in these systems, it is challenging to achieve linearity and symmetry in their current responses, which inevitably degrades ANN accuracy due to inaccurate write-read operations. As a result, memory elements in conventional ReRAM and PCM crossbars are programmed sequentially, limiting their latency to $\sim O(N \times M)$ write cycles, where O is the number of operations. In contrast, a linearly programmable memory would enable arrays that can be updated within a single cycle, resulting in an $O(N \times M)$ advantage and large gains in latency and energy efficiency. For example, using a proof of concept 3 × 3 array of linearly and symmetrically programmable organic ECRAMs (**Figure 2*a*,*b***), Fuller et al. (44) recently demonstrated parallel array programming at high ANN accuracy, while architectural simulations predicted that a 1,024 × 1,024 array would have energy, latency, and area advantages of 476×, 16×, and 9.5×, respectively, compared to an optimized eight-bit static random-access memory accelerator, highlighting the potential of organic synaptic memories in hardware ANNs.

In electrochemical systems in which the conductance state depends mainly on the injection or extraction of ions, a linear increase or decrease in current was achieved in organic

conducting polymers, e.g., PEDOT:PSS (22, 44), and more recently in poly(2-(3,3-bis(2-(2-(2-methoxyethoxy)ethoxy)ethoxy)-[2,2-bithiophen]-5-yl)thieno[3,2-b]thiophene) [p(g2T-TT)] by Melianas et al. (43) (**Figure 2*c,d***). From a semiconductor physics standpoint, this linear behavior is likely related to the filling of the density of states (DoS) of the organic semiconductor upon ion insertion. In general, DoS filling should be such that the change in material conductance (dG) scales linearly with injected ionic charge (dQ) per write pulse. This can be achieved if the material carrier mobility is independent of injected ionic carrier density, as has been recently demonstrated in PEDOT:PSS- and p(g2T-TT)-based ECRAMs exhibiting a linear dG versus dQ response within their operating ranges (43). Most importantly, the linear switching demonstrated by Melianas et al. is attained at high speed (down to 20-ns switching) and with the high endurance ($>10^9$ operations) needed for integration into ANN accelerators.

Other strategies to optimize the linear response of electrochemically gated organic semiconductors are to shift the DoS using chemical additives (54, 55), through synthetic backbone design (56), or by changing the energy level of the reference gate (57, 58). Organic-based ECRAMs are hence promising device candidates for achieving high-quality resistive switching since the redox reactions in the channel can be highly reversible and the same material can be used for both the channel and gate. This reversibility of ion insertion results in other desirable device parameters like high endurance, as we discuss in Section 2.10. These properties contrast with inorganic materials, in which ion insertion may perturb the lattice quite significantly (59).

2.8. Switching Speed

Once a material and the synaptic device made thereof can demonstrate high-quality switching behavior (i.e., linear and highly predictable switching), the next question is, How fast can it switch? The execution of ANN tasks requires fast and repeatable synaptic weight updates. While biological brains, through long-term training and effective synapse-to-synapse transmission, operate in the 1–100-Hz range, such speed is not sufficient for efficient ANN computation using artificial synapses as they lack the massive connectivity and parallelism. In ANN arrays, each synaptic node is required to update the corresponding weight at megahertz frequencies. Such speeds are required for ANN accelerators to compete with the latency of digital ANN implementations utilizing graphics processing units and application-specific integrated circuits.

It has already been demonstrated that inorganic materials have fast switching speeds in synaptic devices (60, 61). The search for, and design of, fast switching organic systems is an emerging and promising field of study (53, 62). For instance, polymer-based ECRAMs have demonstrated ~50-MHz switching speeds (20-ns write pulses) and are predicted to operate faster with further downscaling (43, 44). Modeling predicts that 1- × 1-μm devices will switch faster than 1 GHz using <10 fJ per write (63) (**Figure 2*c,d***). In addition, these devices demonstrated submicrosecond settling time (**Figure 2*e***), i.e., the time it takes for the device conductance to equilibrate following a write pulse, which is critical for achieving low latency in ANN accelerators. This is significantly faster than any inorganic electrochemical memory (millisecond to second settling times) reported to date (64–66). These data demonstrate that organic electronic materials can achieve switching speeds that rival those observed in inorganic resistive switches.

With the ability of organic semiconductors to be tailored both chemically and morphologically, the write-read speeds can be tuned by varying the ionic injection and retention rates. Via side-chain engineering, for instance, ion insertion as well as concomitant backbone doping and dedoping, i.e., conductance modulation, can be tuned in organic electrochemical transistors (OECTs) (67, 68). Indeed, Bischak et al. (69) recently demonstrated that by careful selection of ion-exchange gels, the ionic dynamics and, hence, doping kinetics between biologically relevant aqueous electrolytes

(e.g., K^+) and an otherwise too hydrophobic semiconducting polymer could be tuned. Taking advantage of the structural tunability of organic systems is hence a useful strategy for improving switching dynamics in synaptic memories.

One important materials selection strategy for rapid switching has been the use of small ionic species in electrolyte-gated devices. Additionally, it has been recently proposed that fast switching in organic electrochemical devices occurs when mobile ions are incorporated into the semiconductor channel before electrochemical gating, thereby reducing the ion transit distance and time (70). It was even demonstrated that following deposition of the ion gel electrolyte the channel conductance is affected as a result of ion uptake and passive doping of the semiconducting polymer (43). Intuitively, the surprisingly fast switching (20 ns) in these systems could be associated with very mobile ionic species, more specifically protons. This hypothesis was corroborated when a protic ionic liquid was compared to its aprotic counterpart in solid-state ECRAMs (43). Devices based on the protic ionic liquid performed significantly better. Similar fast dynamics had been previously achieved in PEDOT:PSS-based ECRAMs when using a proton-based electrolyte (22). Novel polymer designs may focus on realizing morphologies and chemical environments favoring the formation of hydrogen-bonded networks to facilitate high-speed Grotthuss transport (71) of protons (or other small ions) in organic devices.

2.9. State Retention

The synaptic weight retention time for specific materials and devices determines suitable applications. In general, there are two main types of applications. The first are dot-product engines, in which the devices are programmed to the desired conductance and are left untouched onward, e.g., the chips in a self-driving car. This type of application requires a retention time of ~10 years, which remains challenging to attain in most organic materials (51) but is possible using inorganic materials. The second is online learning, in which the ANN is constantly learning, e.g., a flying drone that adapts to the changing environment on the fly. In this case, the device conductance (i.e., weights) is constantly updated. These applications don't require long retention, and <1 min can be enough. Shorter retention, such as that used in spiking neural networks in which the device conductance decays following a spike, is outside the scope of this discussion.

Organic-based synaptic devices have repeatedly demonstrated short-term retention. In principle, the device volatility can be inherent to the material, but through device design it has been shown that, for example, by engineering the gating mechanism, the ionic drift in and out of the channel can be strictly controlled by the applied voltage and the spike rate (22, 52, 62, 72). For example, in organic ECRAM devices, by preventing the ions injected into the semiconducting channel from drifting back toward the gate contact, the induced state can be retained until a potential is intentionally applied or undesirable electrical leaks occur. Such control could be achieved in PEDOT:PSS-based ECRAMs in which an additional polymer layer was inserted at the gate-electrolyte interface, like a supercapacitor architecture, thus prohibiting free ion migration after the gate voltage is turned off (22). Using this approach, state retention on the order of minutes has been demonstrated using p(g2T-TT) (43). Such retention was achieved by controlling the capacitive nature of the gate and channel and utilizing a digital switch to regulate the connection between the gate and channel electrodes and to prevent premature ECRAM discharge.

To simplify the architecture of the ECRAM devices, Fuller et al. (44) demonstrated the use of a volatile conductive-bridge memory (CBM) to act as a two-terminal thresholding switch at the PEDOT:PSS gate, constituting an ionic floating-gate (IFG) memory, as shown in **Figure 2*a***. Following programming pulses, the IFG was able to retain its state due to the high OFF resistance ($\sim 10^{12}$) of the CBM switch. Furthermore, in such battery-like ECRAMs, electronically blocking

electrolytes are also sought after as they help prevent any parasitic current flow between the contacts. If state retention is still insufficient, the learned weights can be offloaded to an external inorganic memory for long-term storage.

2.10. Endurance and Environmental Stability

Like conventional computing devices, neuromorphic devices must endure many switching events. Within the array, each synaptic device must operate reliably for a large number of tuning events to reliably execute intended ANN tasks. Therefore, any proposed device should be endurance tested for conductance drift as well as changes in switching characteristics. If the device degrades, the ANN computational accuracy inevitably deteriorates. Typically, computer hardware is designed to last ~10 years. In the case of a training accelerator operating at 1 MHz, the devices should aim for an endurance of 10^{14} switching events (comparable endurance to dynamic random-access memory cells). For inference-only accelerators, $\sim 10^6$ events are expected (for the initial training of the array). In ANNs, parallel programming itself remains challenging; therefore, it is more intuitive to aim for highly durable synaptic devices.

The previously discussed ECRAM examples have demonstrated durable switching behaviors using both PEDOT:PSS and p(g2T-TT) with $>2 \times 10^9$ write-read events (43, 44), which is comparable to the endurance of many emerging inorganic nonvolatile memory devices (73). One of the attractive features found in PEDOT:PSS is that the dedoping and doping process favors (but is not limited to) the insertion and extraction, respectively, of protons, the smallest cationic species. This allows for minimal structural degradation and/or trapping, hence the excellent write-read cycling stability. Such switching behavior was previously utilized by Fuller et al. (44) to demonstrate over 10^8 write-read events and has been exploited in other recent studies, as shown in **Figure 2*e***, accompanied with the rapid switching discussed above (43).

Other polymer systems have been investigated especially owing to their open structure, which allows for facile ionic intercalation. Such open structure allows for the insertion of large ionic species, for instance, using gel electrolytes such as 1-ethyl-3-methylimidazolium bis(trifluoromethylsulfonyl)amide in the case of P3HT, thus enabling stable writing and erasing in all-solid-state memory devices (74). PEDOT:PSS-based synaptic devices have also been demonstrated to stably modulate over a large number of events whether in liquid electrolytes (e.g., aqueous KCl) or gel electrolytes (22, 44, 75). Once again, the optimization of electrolyte and film morphology is crucial for the realization of highly durable organic devices. Additional considerations that are typically relevant in other electronic devices are the selection of dopants (76), moisture affinity (not necessarily a challenge depending on the operating environment), and interface engineering.

The operational environment must be considered when benchmarking the endurance of a neuromorphic device. Since any device inevitably heats up during operation due to Joule heating, as well as due to the heating of peripheral electronics in the case of monolithic integration with silicon electronics, the device operating temperature must be considered in its design to account for internal and external heating. In addition, the chemical (humidity, oxygen, etc.) environment in which the device operates must also be considered. For example, materials that require a certain humidity to operate well (e.g., proton-conducting electrolytes) are not well suited for integration into an ANN accelerator, since standard electronics packaging inevitably leads to dry conditions and thus limits device performance. As a result, the device properties should ideally be benchmarked versus intended use and environmental conditions (humidity, temperature, etc.). In that regard, novel designs for electrolytes, conducting materials, and encapsulation techniques should also be considered. In fact, in the study by Melianas et al. (43), ECRAM devices based on

p(g2T-TT) could reliably function under elevated temperatures and dry conditions, which is typically highly challenging when employing proton conductors as their performance rapidly deteriorates when not properly hydrated. Under such conditions, these devices also exhibited durable switching behaviors. Not only does this work demonstrate the ability of organic-based memory devices to be sufficiently durable once implemented in existing circuitries, but it also shows the potential enhancement in neuromorphic performance via novel polymer designs beyond PEDOT:PSS.

Additionally, environmental oxygen presents a challenge for operating organic neuromorphic devices due to the instability of many organic semiconductors to oxidation. One approach to avoid parasitic reactions with oxygen in PEDOT:PSS-based devices is to introduce chemical dopants that act as reducing agents to stabilize the reduced state of PEDOT (55). Additionally, encapsulation methods can be utilized to reduce the presence of oxygen at the device interface. Another strategy for organic materials is to design polymers with deeper ionization potential (p type) or electron affinity (n type) to make oxidation reactions unfavorable. Giovannitti et al. (56) demonstrated that by synthesizing a polymer backbone consisting of a pyridine-flanked diketopyrrolopyrrole unit and a 3,3′-methoxybithiophene unit, the polymer was highly stable in air and avoided parasitic oxidation. These examples demonstrate the unique advantages of the tunable nature of organic semiconductors for improved endurance and environmental stability.

2.11. Back-End-of-Line Compatibility

For large-scale integration with CMOSs, organic devices must withstand semiconductor foundry conditions. More specifically, the devices must at the very least withstand up to an ∼400°C anneal during the BEOL portion of integrated circuit fabrication. Though organic materials can be molecularly tailored or engineered to withstand most steps in nanofabrication, thermal durability remains one of the most challenging requirements. Thermogravimetric analysis and differential scanning calorimetry are commonly used to assess the thermal stability of organic materials. Though several conjugated systems exhibit thermal degradation at temperatures as high as 500°C, systematic analysis of the electronic properties after such harsh thermal exposure is rarely carried out. For organic synaptic devices, all components must be able to withstand foundry temperatures without jeopardizing the device integrity and performance. This remains challenging as most successful active materials, e.g., PEDOT:PSS, exhibit decomposition temperatures around 300°C (77). The bottleneck in this case is not only whether the thin film can survive the harsh thermal conditions, but also whether the formed crystalline domains can maintain their microstructural integrity during subsequent resistive switching, e.g., following ion insertion (78).

Recent studies have demonstrated the use of high-T_g insulating matrices as rigid hosts to process thermally robust semiconducting composites into thin films (79, 80). In addition, semiconducting polymers are structurally tunable to attain properties including thermal stability (81). These approaches show that there might be processing strategies for stable semiconducting systems. Common molecular considerations for thermal robustness include the use of highly fused systems, therefore minimizing any rotational freedom and backbone planarity; increasing the molecular weight; cross-linking; and addition of pendant groups (81). Such strategies are envisioned to allow organic semiconductors to withstand extreme heat and could ensure compliance of organic synaptic devices with BEOL processing. Further research efforts in that regard are warranted as no organic-based device has yet demonstrated compliance with foundry conditions.

In addition to the semiconducting channel stability, the electrolyte must also survive the baking steps. Several demonstrations of organic synaptic devices we have discussed utilized ionic liquid in gel electrolytes. Ionic liquids, though molten at room temperature, have been reported to be

stable up to 400°C (82, 83), but they are typically infused in gels that soften at high temperatures, affecting their mechanical integrity. Corresponding gel electrolytes are obtained using thermally robust Teflon-like matrices (43), but it remains to be investigated whether such systems also enable the high-performance synaptic behaviors discussed above (e.g., high speed, linearity, endurance) With reported thermal stability of individual components, the obvious next step is to conduct thermal annealing tests on fully assembled devices and analyze their layer-to-layer integrity as well as electrical performance after exposure to BEOL conditions. Ultimately, BEOL compatibility appears to be the most challenging requirement if the designed synaptic devices are intended for high-performance neuromorphic computing.

While it may be feasible to achieve most of the metrics discussed above, e.g., as demonstrated in organic-based ECRAMs, competing in the area of high-performance computing remains challenging for organic devices due to the technological maturity of inorganic technologies. To a large extent, the difficulty for organic materials arises due to the need to achieve both high performance and scaling to technologically relevant submicrometer scales, all while maintaining compatibility with semiconductor foundry fabrication processes. While several reports have indicated promising progress to address these challenges, further studies are needed to meet all the stringent neuromorphic device requirements in a single organic material or device system.

Despite the challenges facing organic electronic materials in the area of high-performance neuromorphic computing, they offer unique opportunities owing to their intrinsic biocompatibility, which is attainable in inorganic materials only via engineering strategies (84). Due to this advantage, we therefore argue that a yet largely untapped potential of organic neuromorphic devices lies in bioelectronics applications. Having equipped the reader with the general device requirements for computing applications, we now shift our focus to more biologically oriented applications, in which many of the before-mentioned requirements are less stringent and a new set of requirements emerges.

3. BIOINTERFACING

In addition to devices for ANN accelerators, organic semiconducting materials and the resulting electronic devices have recently been demonstrated as great candidates for interfacing with biological tissues for sensing, medical, neuro-prosthetic, and other bioelectronics applications (85, 86). In particular, the ion-gated organic materials discussed above have shown excellent properties for integration with tissue due to their water stability, low-voltage operation, soft mechanical properties, and ability to convert ion/chemical signals in solution to electronic signals (86). Because these materials can achieve the biocompatibility required for biotic/abiotic interfaces and have unique properties that allow them to emulate the biological synapses, there has been increasing interest in utilizing organic materials for directly integrating ANNs with biomedical devices. As discussed in the introduction, integrating ANNs with implantable devices has the potential to enable adaptable prosthetic or robotic devices that are tailored to the individual user (87). We envision that ANN integrated systems could augment or replace functional systems in patients suffering from irreparable trauma, specifically damage to neural tissue. In this section, we discuss the current work aimed at integrating neuromorphic devices with biological tissue and give an outlook on the opportunities and materials strategies in these areas for organic materials.

There are a wide range of approaches to coupling between devices and biological neural networks. One approach is to utilize functional materials that can replicate the response of living matter and directly stimulate the surrounding neural tissue. This approach is exemplified by the work of Maya-Vetencourt et al. (88) in which they utilize a silk-PEDOT:PSS-P3HT photo-responsive prosthesis implanted in the retina of rats with retinal dystrophy to directly

stimulate the optic nerve. This direct conversion of the natural light stimulus captured by the eye to a photovoltage that could stimulate the nerve tissue demonstrated successful partial restoration of sight (persisting up to 10 months after surgery) in the dystrophic rats. In later work, the authors adapted their device by utilizing injectable P3HT nanoparticles to avoid the surgical implantation of the prosthetic device (89). While this approach is highly promising, one of the remaining challenges is to capture the complex functionality of the specific retinal cells to better emulate and restore biological visual mechanics.

Another approach is to use ANNs to preprocess incoming signals and perform subsequent actions tailored to the unique characteristics of the user or system. For instance, Schwemmer et al. (33) demonstrated that brain-computer interfaces for repairing motor function could be significantly enhanced by using a neural network to interpret the electrical signals from a microelectrode array implanted in the motor cortex. Using a transferred neural network model, the participant, whose hand and arm were paralyzed due to a spinal cord injury, was able to train the network to recognize brain signals corresponding to the desired hand motions. Furthermore, by utilizing functional electrical stimulation on the participant's forearm, the paralyzed hand was reanimated in real time as a response to the participant's brain activity, showing the potential to restore cortical-motor functionality. However, this approach is limited to lab-scale experiments due to the poor chronic stability of silicon-based recording devices (90) and the bulky electronics required to run the ANN algorithm. Similarly, Taunyazov et al. (91) demonstrated how ANNs can be utilized to emulate event-driven perception using visual and tactile sensors for robotics. The authors utilized sensors that output spike encoded signals (92) and fed them into a spiking neural network model to enable real-time learning and response in a robotic arm. Similar systems integrated with biological tissue can be envisioned for bioinspired prosthetic interfaces (93).

To build up these neuro-inspired systems, it is critical to start at the individual device level. While the performance metrics for neuroinspired bioelectronic devices are not as straightforward as for neuromorphic devices in ANN accelerators, we offer some strategies to follow for utilizing organic materials. First, the biocompatibility of the device itself should be assessed for long-term stability in implantable interfaces. Second, the device should offer some biological functionality, such as synaptic plasticity, sensory perception, chemical sensitivity, or neural stimulation, that can be utilized in the context of the biotic/abiotic interface. In the rest of this section, we use examples from the literature to highlight unique approaches for utilizing organic materials for biointerfacing neuromorphic devices.

Organic synaptic devices have repeatedly demonstrated stimulus-responsive brain-inspired functions (94). For instance, organic electrochemical synaptic devices have been shown to mediate and modulate communication between living biological cells and respond to external stimuli (95, 96). Using PANI- or PEDOT:PSS-based electrochemical devices, biological stimuli were used to condition or train artificial synapses, mimicking communication between neurons in the brain. More specifically, the first evidence of unidirectional, activity-dependent coupling of two live neurons in brain slices via organic memristive devices (OMDs) was demonstrated, as shown in **Figure 3*a*,*b*** (97). The OMD used was a polymeric electrochemical element with hysteresis and rectifying features. OMD coupling with the live cells was facilitated by tuning and control of its resistance via neuronal activity and the excitation threshold in the postsynaptic neuron as shown in **Figure 3*c***.

Likewise, other research groups have extensively shown that OECTs that respond to biologically relevant ions are excellent candidates for biointerfacing (23, 75, 98, 99). OECTs use an electrolyte to modulate the conductance state of the channel via the migration of ionic species, typically in response to a small potential change (100). These devices are thus able to emulate the ion flux–driven synaptic activity found in biological systems. Owing to the creation of an internal

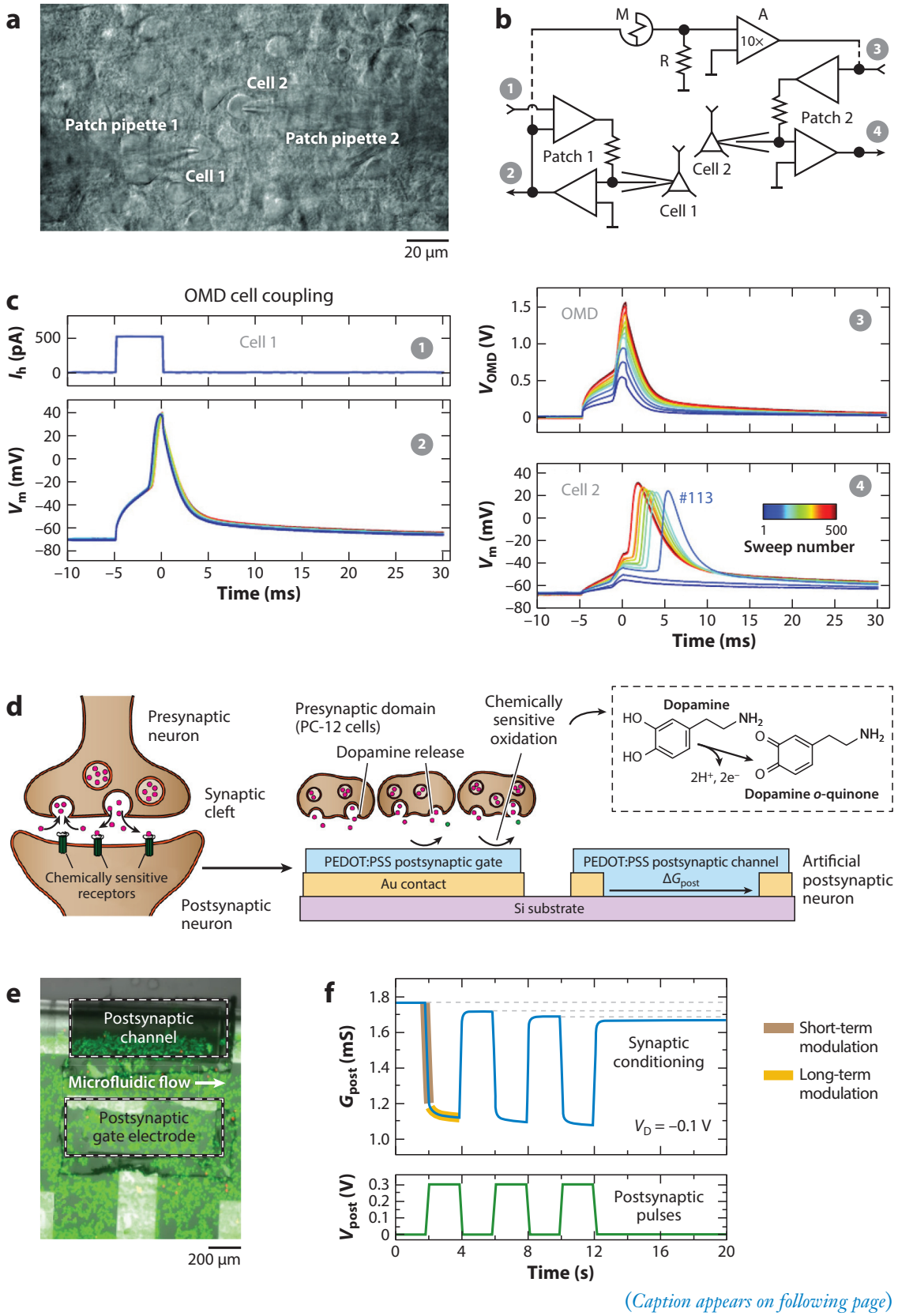

(Caption appears on following page)

Figure 3 (*Figure appears on preceding page*)

The road toward neurotransmitter-mediated biomachine interfacing. (*a*) Infrared differential interference contrast microphotograph of a P7 rat brain slice with visually identified L5/6 neocortical cells (cells 1 and 2) recorded simultaneously. (*b*) Electrical scheme of two patch-clamp amplifier head stages (patch 1 and patch 2), (❶,❸) patch-clamp holding inputs and (❷,❹) patch-clamp primary outputs, and an OMD-based circuit (5 × 5 mm) connecting two neurons. (*c*) Traces of current-clamp recordings from cells 1 and 2 before (*left*) (89) and after (*right*) OMD coupling. Panels *a–c* adapted with permission from Reference 97. (*d*) Device design utilizing biological inputs, i.e., dopamine release from living neuroendocrine cells. (*e*) Micrographs demonstrating live cells on a PEDOT:PSS-based artificial synapse. (*f*) Demonstration of short-term and long-term modulation in the postsynaptic current in response to dopamine oxidation. Panels *d–f* adapted with permission from Reference 102; copyright 2020 Springer Nature. Abbreviations: A, amplifier; M, memristive device; OMD, organic memristive device; PEDOT:PSS, poly[3,4-(ethylenedioxy)thiophene]: poly(styrene sulfonate); R, resistor.

electric double layer, these devices are inherently capacitive, which leads to low noise, minimal leakage currents, low operating voltages, and high gain. Additionally, the lack of glial response to flexible OECT-based electrocorticography recording electrode arrays is a demonstration of their biocompatibility (101). Their simplified device architecture, mode of operation, scalability, and ability to be interconnected through a common gate or electrolyte (75, 98, 99) also make OECTs an attractive device architecture for integrated bioelectronics. Such features are promising in designing artificial perceptron systems that can complement and even mimic biological sensory systems. These devices would enable synaptic training using biological signals, such as chemical neurotransmitters, light, and pressure.

In biological systems, it is common that neurons communicate via the release and detection of chemical neurotransmitters. Synaptic activity and the inherent neural connectivity result from the occurrence of such chemical signaling. To enable the interfacing between neuromorphic devices and biological cells, it is important to demonstrate synaptic conditioning based on these chemical signals. Keene et al. (102) recently demonstrated a biohybrid synapse with neurotransmitter-mediated plasticity that enabled synaptic conditioning in response to dopamine, a prominent neurotransmitter linked to conditioning in the brain (103). In this work, PC-12 neuroendocrine cells were plated onto an organic neuromorphic device, which acted as a postsynapse via a microfluidic channel. The PC-12 cell layer served as a presynaptic domain that spontaneously released dopamine molecules onto the gate interface of the PEDOT:PSS-based postsynapse (**Figure 3*d***). By controlling the dopamine recycling with microfluidic flow, the doping state of the polymer in the channel could be conditioned in response to charges freed by the oxidation of dopamine into its quinone form, a behavior that emulates dopamine secretion in synaptic clefts (**Figure 3*e*,*f***). It was shown that the presence of dopamine not only dedopes (i.e., injects electrons into) the channel upon a postsynaptic potential, but also enables long-term state retention. Other studies have also demonstrated such short-term plasticity of PEDOT:PSS in response to dopamine in a two-terminal device configuration (72). In combination with the fast response, i.e., short-term plasticity, this dopamine-dependent long-term potentiation showed that the hybrid device can emulate Hebbian learning, a path toward ANNs and adaptive biological interfaces.

A feedback process between a sensory receptor, a motor unit, and an artificial neuron is sought when targeting machine learning applications (104). Light, sound, temperature, gases, liquids, and pressure are the common environmental stimuli that trigger the peripheral nervous system, which can in turn transmit the generated action potentials onto the central nervous system and determine behavior (94). To ensure low latency in robotics and prosthetics applications, the sensory units should be equipped with hardware ANNs to process the data on site and in real time, before subsequent data transfer to the motor units. By directly integrating hardware ANNs,

such devices could run independently of external connections (e.g., WiFi, Bluetooth), potentially enabling lower latency and energy costs for data processing. For instance, to sense light and react accordingly, Lee et al. (104) demonstrated an organic optoelectronic sensorimotor synapse. By bridging an organic optoelectronic synapse and a neuromuscular system based on a stretchable organic nanowire synaptic transistor, the authors could mimic the biological response to light. A photodetector was used as the sensory unit, from which voltages could be generated in response to optical spikes. The generated potential pulses were then used to drive a stretchable synaptic transistor device, which could then be trained to drive a polymer actuator device. The synaptic transistor was designed to be fully stretchable and extremely soft by using ultrastretchable styrene ethylene butylene styrene as the substrate and carbon nanotube wires (CNWs) as source and drain contacts. A stretchable active channel was achieved by using semiconducting nanowires made of an electro-spun blend of a fused-thiophene diketopyrrolopyrrole-conjugated polymer and PEO. To drive the synaptic device, a soft gel based on poly(styrene-b-methyl methacrylate-b-styrene) triblock copolymer and 1-ethyl-3-methylimidazolium bis(trifluoromethylsulfonyl)imide ionic liquid was used as the electrolyte. The use of all-stretchable polymer components enabled such transistor devices to be stretchable up to 100% with no degradation in electronic performance. More impressive was the synaptic plasticity demonstrated in these devices, even under 100% strain. The stretchable nature of these devices enables their integration with moving tissue, such as in muscles or on the skin, without significant mechanical degradation due to strain cycling.

The conductance of the CNW device showed a spike duration–dependent plasticity and a spike number–dependent plasticity, which are learning behaviors found in natural systems. Such learning behavior could be used to contract and extend a polymer-based actuator emulating muscular functions to perform tapping-like tasks such as communicating in Morse code (**Figure 4*a*,*b***). This closed-loop system is thus an excellent example of mimicking muscle movement (e.g., blinking) in response to light after training or synaptic conditioning. In such circuit designs, the organic synaptic transistor is the processing center of the loop. On the one hand, it is envisioned that biological photoreceptors can interface with artificial synapses, enabling applications in vision correction, such as by enhancing the specificity of stimulation of the optic nerve. On the other hand, artificial synapses can also be used to directly interface and drive biological muscles—a possible research direction for organic-based smart prosthetics.

In a recent article by Kim et al. (105), a synaptic transistor coupled with a pressure sensor and a ring oscillator was reported to emulate the functions of a biological afferent nerve. In this design, an array of pressure sensors mimicking animal skin was utilized to capacitively tune the output voltage in response to touch. The generated pulses were then processed through a series of ring oscillators before being used to modulate the conductance state within the channel of an organic synaptic transistor (**Figure 4*b*,*c***). The ring oscillators allowed for the programming of the synaptic transistor to function as an adder when multiple pressure pulses were applied, thus emulating dendrite connectivity found in biological neurons in which multiple presynaptic action potentials from separate somatotopic coordinates are commonly summed (106). The measured postsynaptic currents in the memory unit exhibited a pressure-dependent plasticity as well as a time-dependent plasticity, which are learning behaviors found in biological afferent nerves. The current retention times were also found to be in a similar range as the biological systems (milliseconds) (80). These artificial learning behaviors were used to stimulate the afferent nerve of a cockroach by placing the device onto the animal. Using this approach, leg muscle movement was artificially controlled in response to external pressures (**Figure 4*c*,*d***). This seamless integration of sensory detection and stimulation has the potential to enable prosthetic devices that augment or replace functionality in living systems.

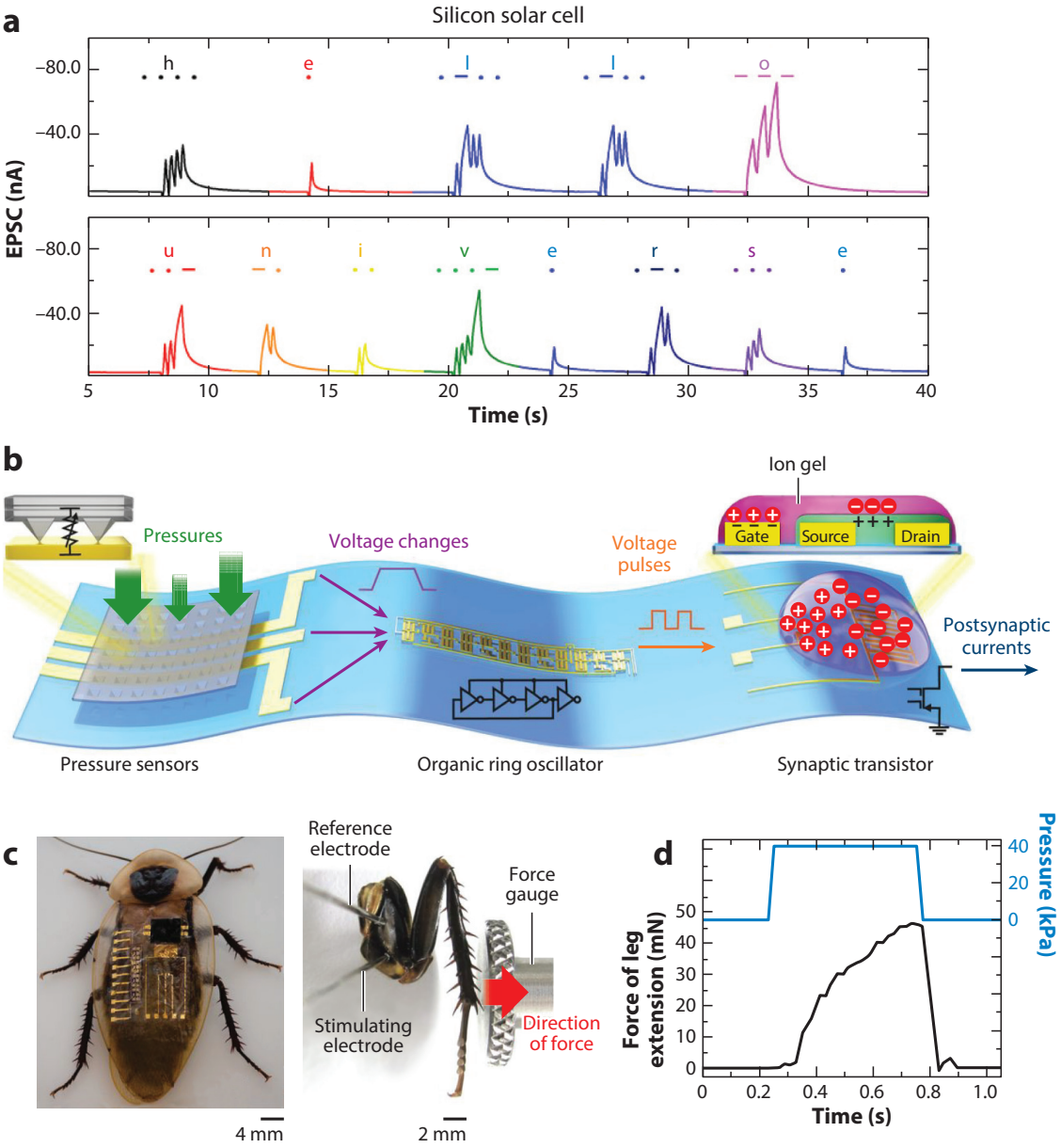

Figure 4

(*a*) IR (*top*) and UV light (*bottom*)–triggered current amplitudes of an organic nanowire synaptic transistor with the International Morse code of "hello universe." Panel *a* adapted with permission from Reference 104; copyright The Authors, some rights reserved; exclusive licensee American Association for the Advancement of Science (CC BY-NC 4.0). (*b*) Design of a bioinspired afferent nerve. (*c*) Photographs of the artificial afferent nerve patched onto the animal's back and the electrodes on a detached cockroach leg to detect the response to external pressure. (*d*) Measured force as a response from the animal's leg extension as a function of applied pressure. Panels *b–d* adapted with permission from Reference 105. Abbreviation: EPSC, excitatory postsynaptic current.

4. CLOSING REMARKS AND OUTLOOK

We have discussed materials design strategies and highlighted that in recent years organic materials have emerged as promising candidates for neuromorphic computing applications. In addition to realizing high performance in ANN accelerators, organic semiconductors have been shown to be biocompatible, which is attractive for machine-body interfacing applications, and

offer some competitive advantages compared to currently used inorganic materials, owing to their chemical tunability. We highlighted general design strategies to address the remaining challenges facing organic neuromorphic devices for high-performance neuromorphic computing as well as biointerfacing applications. For high-performance computing, the main challenge lies in realizing submicrometer-sized devices while retaining favorable performance (programming linearity, fast switching, low operating current and voltage, low switching energy, high endurance, low device-to-device variability, etc.) and improving BEOL compliance for large-scale integration of ANN accelerators with CMOS circuitry. Since these requirements are significantly less stringent for bio-related applications, we propose biointerfacing as a promising future research direction for organic neuromorphic devices, owing to their biocompatibility, softness, and tunability by chemical synthesis. For biointerfacing, the devices must be biocompatible to ensure long-term stability in implantable interfaces and must enable some biological functionality, such as synaptic plasticity in response to biological signals, e.g., following neurotransmitter release. The demonstration of biointegrated and high-performance computing devices is envisioned to revolutionize areas such as healthcare, entertainment, and smart textiles, to name a few, and is a leap that organic neuromorphic devices are uniquely poised to take in the near future.

DISCLOSURE STATEMENT

The authors are not aware of any affiliations, memberships, funding, or financial holdings that might be perceived as affecting the objectivity of this review.

ACKNOWLEDGMENTS

A.G. acknowledges support from a postdoctoral fellowship from the Geballe Laboratory for Advanced Materials (GLAM) at Stanford University. A.M. acknowledges support from the Knut and Alice Wallenberg Foundation (KAW 2016.0494) for postdoctoral research at Stanford University. A.S. and S.T.K. acknowledge financial support from the National Science Foundation and the Semiconductor Research Corporation (E2CDA award 1739795). Additionally, S.T.K. acknowledges the Stanford Graduate Fellowship fund for support.

LITERATURE CITED

1. Mead C. 1990. Neuromorphic electronic systems. *Proc. IEEE* 78:1629–36
2. Bliss TVP, Collingridge GL. 1993. A synaptic model of memory: long-term potentiation in the hippocampus. *Nature* 361:31–39
3. Strukov DB, Snider GS, Stewart DR, Williams RS. 2008. The missing memristor found. *Nature* 453:80–83
4. Yang JJ, Strukov DB, Stewart DR. 2013. Memristive devices for computing. *Nat. Nanotechnol.* 8:13–24
5. Jeong DS, Kim KM, Kim S, Choi BJ, Hwang CS. 2016. Memristors for energy-efficient new computing paradigms. *Adv. Electron. Mater.* 2:1600090
6. Sun J, Fu Y, Wan Q. 2018. Organic synaptic devices for neuromorphic systems. *J. Phys. D Appl. Phys.* 51:314004
7. Zidan MA, Strachan JP, Lu WD. 2018. The future of electronics based on memristive systems. *Nat. Electron.* 1:22–29
8. Cho B, Song S, Ji Y, Kim T-W, Lee T. 2011. Organic resistive memory devices: performance enhancement, integration, and advanced architectures. *Adv. Funct. Mater.* 21:2806–29
9. Hickmott TW. 1962. Low-frequency negative resistance in thin anodic oxide films. *J. Appl. Phys.* 33:2669–82
10. Hickmott TW. 1964. Potential distribution and negative resistance in thin oxide films. *J. Appl. Phys.* 35:2679–89

11. Choi BJ, Torrezan AC, Strachan JP, Kotula PG, Lohn AJ, et al. 2016. High-speed and low-energy nitride memristors. *Adv. Funct. Mater.* 26:5290–96
12. Govoreanu B, Kar GS, Chen Y, Paraschiv V, Kubicek S, et al. 2011. $10\times10nm^2$ Hf/HfOx crossbar resistive RAM with excellent performance, reliability and low-energy operation. In *2011 International Electron Devices Meeting*, pp. 31.6.1–4. Piscataway, NJ: IEEE
13. Benjamin BV, Gao P, McQuinn E, Choudhary S, Chandrasekaran AR, et al. 2014. Neurogrid: a mixed-analog-digital multichip system for large-scale neural simulations. *Proc. IEEE* 102:699–716
14. Davies M, Srinivasa N, Lin T, Chinya G, Cao Y, et al. 2018. Loihi: a neuromorphic manycore processor with on-chip learning. *IEEE Micro* 38:82–99
15. Merolla PA, Arthur JV, Alvarez-Icaza R, Cassidy AS, Sawada J, et al. 2014. A million spiking-neuron integrated circuit with a scalable communication network and interface. *Science* 345:668–73
16. Li S, Zeng F, Chen C, Liu H, Tang G, et al. 2013. Synaptic plasticity and learning behaviours mimicked through Ag interface movement in an Ag/conducting polymer/Ta memristive system. *J. Mater. Chem. C* 1:5292–98
17. Wu S, Tsuruoka T, Terabe K, Hasegawa T, Hill JP, et al. 2011. A polymer-electrolyte-based atomic switch. *Adv. Funct. Mater.* 21:93–99
18. Park Y, Lee J-S. 2017. Artificial synapses with short- and long-term memory for spiking neural networks based on renewable materials. *ACS Nano* 11:8962–69
19. Wang L, Wang Z, Lin J, Yang J, Xie L, et al. 2016. Long-term homeostatic properties complementary to Hebbian rules in CuPc-based multifunctional memristor. *Sci. Rep.* 6:35273
20. Wang H, Meng F, Cai Y, Zheng L, Li Y, et al. 2013. Sericin for resistance switching device with multilevel nonvolatile memory. *Adv. Mater.* 25:5498–503
21. Kim DH, Kim WK, Woo SJ, Wu C, Kim TW. 2017. Highly-reproducible nonvolatile memristive devices based on polyvinylpyrrolidone: graphene quantum-dot nanocomposites. *Org. Electron.* 51:156–61
22. van de Burgt Y, Lubberman E, Fuller EJ, Keene ST, Faria GC, et al. 2017. A non-volatile organic electrochemical device as a low-voltage artificial synapse for neuromorphic computing. *Nat. Mater.* 16:414–18
23. Gkoupidenis P, Schaefer N, Garlan B, Malliaras GG. 2015. Neuromorphic functions in PEDOT:PSS organic electrochemical transistors. *Adv. Mater.* 27:7176–80
24. Bandyopadhyay A, Sahu S, Higuchi M. 2011. Tuning of nonvolatile bipolar memristive switching in Co(III) polymer with an extended azo aromatic ligand. *J. Am. Chem. Soc.* 133:1168–71
25. Dong WS, Zeng F, Lu SH, Liu A, Li XJ, Pan F. 2015. Frequency-dependent learning achieved using semiconducting polymer/electrolyte composite cells. *Nanoscale* 7:16880–89
26. Yang X, Wang C, Shang J, Zhang C, Tan H, et al. 2016. An organic terpyridyl-iron polymer based memristor for synaptic plasticity and learning behavior simulation. *RSC Adv.* 6:25179–84
27. Xu W, Cho H, Kim Y-H, Kim Y-T, Wolf C, et al. 2016. Organometal halide perovskite artificial synapses. *Adv. Mater.* 28:5916–22
28. Tress W. 2017. Metal halide perovskites as mixed electronic–ionic conductors: challenges and opportunities—from hysteresis to memristivity. *J. Phys. Chem. Lett.* 8:3106–14
29. Fuller EJ, Li Y, Bennet C, Keene ST, Melianas A, et al. 2019. Redox transistors for neuromorphic computing. *IBM J. Res. Dev.* 63:9:1–9:9
30. van de Burgt Y, Melianas A, Keene ST, Malliaras G, Salleo A. 2018. Organic electronics for neuromorphic computing. *Nat. Electron.* 1:386–97
31. Esteva A, Kuprel B, Novoa RA, Ko J, Swetter SM, et al. 2017. Dermatologist-level classification of skin cancer with deep neural networks. *Nature* 542:115–18
32. Stephansen JB, Olesen AN, Olsen M, Ambati A, Leary EB, et al. 2018. Neural network analysis of sleep stages enables efficient diagnosis of narcolepsy. *Nat. Commun.* 9:5229
33. Schwemmer MA, Skomrock ND, Sederberg PB, Ting JE, Sharma G, et al. 2018. Meeting brain–computer interface user performance expectations using a deep neural network decoding framework. *Nat. Med.* 24:1669–76
34. Martin SJ, Grimwood PD, Morris RGM. 2000. Synaptic plasticity and memory: an evaluation of the hypothesis. *Annu. Rev. Neurosci.* 23:649–711
35. Whitlock JR, Heynen AJ, Shuler MG, Bear MF. 2006. Learning induces long-term potentiation in the hippocampus. *Science* 313:1093–97

36. Cosemans S, Verhoef B, Doevenspeck J, Papistas IA, Catthoor F, et al. 2019. Towards 10000TOPS/W DNN inference with analog in-memory computing—a circuit blueprint, device options and requirements. In *2019 IEEE International Electron Devices Meeting (IEDM)*, pp. 22.2.1–4. Piscataway, NJ: IEEE
37. Hasegawa T, Ohno T, Terabe K, Tsuruoka T, Nakayama T, et al. 2010. Learning abilities achieved by a single solid-state atomic switch. *Adv. Mater.* 22:1831–34
38. Pickett MD, Medeiros-Ribeiro G, Williams RS. 2013. A scalable neuristor built with Mott memristors. *Nat. Mater.* 12:114–17
39. Salinga M, Kersting B, Ronneberger I, Jonnalagadda VP, Vu XT, et al. 2018. Monatomic phase change memory. *Nat. Mater.* 17:681–85
40. Goswami S, Matula AJ, Rath SP, Hedström S, Saha S, et al. 2017. Robust resistive memory devices using solution-processable metal-coordinated azo aromatics. *Nat. Mater.* 16:1216–24
41. Xu W, Min S-Y, Hwang H, Lee T-W. 2016. Organic core-sheath nanowire artificial synapses with femtojoule energy consumption. *Sci. Adv.* 2:e1501326
42. Tang J, Bishop D, Kim S, Copel M, Gokmen T, et al. 2018. ECRAM as scalable synaptic cell for high-speed, low-power neuromorphic computing. In *2018 IEEE International Electron Devices Meeting (IEDM)*, pp. 13.1.1–4. Piscataway, NJ: IEEE
43. Melianas A, Quill TJ, LeCroy G, Tuchman Y, Loo HV, et al. 2020. Temperature-resilient solid-state organic artificial synapses for neuromorphic computing. *Sci. Adv.* 6:eabb2958
44. Fuller EJ, Keene ST, Melianas A, Wang Z, Agarwal S, et al. 2019. Parallel programming of an ionic floating-gate memory array for scalable neuromorphic computing. *Science* 364:570–74
45. Jang S, Jang S, Lee E-H, Kang M, Wang G, Kim T-W. 2019. Ultrathin conformable organic artificial synapse for wearable intelligent device applications. *ACS Appl. Mater. Interfaces* 11:1071–80
46. Mainzer K. 2013. Local activity principle: The cause of complexity and symmetry breaking. In *Chaos, CNN, Memristors and Beyond*, ed. A Adamatzky, G Chen, pp. 146–59. Singapore: World Sci.
47. Agarwal S, Plimpton SJ, Hughart DR, Hsia AH, Richter I, et al. 2016. Resistive memory device requirements for a neural algorithm accelerator. In *2016 International Joint Conference on Neural Networks*, pp. 929–38. Piscataway, NJ: IEEE
48. Yang B, Lu Y, Jiang D, Li Z, Zeng Y, et al. 2020. Bioinspired multifunctional organic transistors based on natural chlorophyll/organic semiconductors. *Adv. Mater.* 32:2001227
49. Dai S, Wu X, Liu D, Chu Y, Wang K, et al. 2018. Light-stimulated synaptic devices utilizing interfacial effect of organic field-effect transistors. *ACS Appl. Mater. Interfaces* 10:21472–80
50. Wang T-Y, He Z-Y, Chen L, Zhu H, Sun Q-Q, et al. 2018. An organic flexible artificial bio-synapses with long-term plasticity for neuromorphic computing. *Micromachines* 9:239
51. Nguyen VC, Lee PS. 2016. Coexistence of write once read many memory and memristor in blend of poly(3,4-ethylenedioxythiophene):polystyrene sulfonate and polyvinyl alcohol. *Sci. Rep.* 6:38816
52. Prudnikov NV, Lapkin DA, Emelyanov AV, Minnekhanov AA, Malakhova YN, et al. 2020. Associative STDP-like learning of neuromorphic circuits based on polyaniline memristive microdevices. *J. Phys. D Appl. Phys.* 53:414001
53. Leydecker T, Herder M, Pavlica E, Bratina G, Hecht S, et al. 2016. Flexible non-volatile optical memory thin-film transistor device with over 256 distinct levels based on an organic bicomponent blend. *Nat. Nanotechnol.* 11:769–75
54. Keene ST, van der Pol TPA, Zakhidov D, Weijtens CHL, Janssen RAJ, et al. 2020. Enhancement-mode PEDOT:PSS organic electrochemical transistors using molecular de-doping. *Adv. Mater.* 32:2000270
55. Keene ST, Melianas A, van de Burgt Y, Salleo A. 2019. Mechanisms for enhanced state retention and stability in redox-gated organic neuromorphic devices. *Adv. Electron. Mater.* 5:1800686
56. Giovannitti A, Rashid RB, Thiburce Q, Paulsen BD, Cendra C, et al. 2020. Energetic control of redox-active polymers toward safe organic bioelectronic materials. *Adv. Mater.* 32:1908047
57. Doris SE, Pierre A, Street RA. 2018. Dynamic and tunable threshold voltage in organic electrochemical transistors. *Adv. Mater.* 30:1706757
58. Kergoat L, Herlogsson L, Piro B, Pham MC, Horowitz G, et al. 2012. Tuning the threshold voltage in electrolyte-gated organic field-effect transistors. *PNAS* 109:8394–99
59. Wu H, Chan G, Choi JW, Ryu I, Yao Y, et al. 2012. Stable cycling of double-walled silicon nanotube battery anodes through solid–electrolyte interphase control. *Nat. Nanotechnol.* 7:310–15

60. Pickett MD, Williams RS. 2012. Sub-100 fJ and sub-nanosecond thermally driven threshold switching in niobium oxide crosspoint nanodevices. *Nanotechnology* 23:215202
61. Lanza M, Wong H-SP, Pop E, Ielmini D, Strukov D, et al. 2019. Recommended methods to study resistive switching devices. *Adv. Electron. Mater.* 5:1800143
62. Battistoni S, Erokhin V, Iannotta S. 2019. Frequency driven organic memristive devices for neuromorphic short term and long term plasticity. *Org. Electron.* 65:434–38
63. Keene ST, Melianas A, Fuller EJ, van de Burgt Y, Talin AA, Salleo A. 2018. Optimized pulsed write schemes improve linearity and write speed for low-power organic neuromorphic devices. *J. Phys. D Appl. Phys.* 51:224002
64. Fuller EJ, Gabaly FE, Léonard F, Agarwal S, Plimpton SJ, et al. 2017. Li-ion synaptic transistor for low power analog computing. *Adv. Mater.* 29:1604310
65. Kim S, Todorov T, Onen M, Gokmen T, Bishop D, et al. 2019. Metal-oxide based, CMOS-compatible ECRAM for deep learning accelerator. In *2019 IEEE International Electron Devices Meeting (IEDM)*, pp. 35.7.1–4. Piscataway, NJ: IEEE
66. Li Y, Fuller EJ, Asapu S, Agarwal S, Kurita T, et al. 2019. Low-voltage, CMOS-free synaptic memory based on Li*X*TiO$_2$ redox transistors. *ACS Appl. Mater. Interfaces* 11:38982–92
67. Giovannitti A, Sbircea D-T, Inal S, Nielsen CB, Bandiello E, et al. 2016. Controlling the mode of operation of organic transistors through side-chain engineering. *PNAS* 113:12017–22
68. Giovannitti A, Maria IP, Hanifi D, Donahue MJ, Bryant D, et al. 2018. The role of the side chain on the performance of n-type conjugated polymers in aqueous electrolytes. *Chem. Mater.* 30:2945–53
69. Bischak CG, Flagg LQ, Ginger DS. 2020. Ion exchange gels allow organic electrochemical transistor operation with hydrophobic polymers in aqueous solution. *Adv. Mater.* 32:2002610
70. Spyropoulos GD, Gelinas JN, Khodagholy D. 2019. Internal ion-gated organic electrochemical transistor: a building block for integrated bioelectronics. *Sci. Adv.* 5:eaau7378
71. Wu X, Hong JJ, Shin W, Ma L, Liu T, et al. 2019. Diffusion-free Grotthuss topochemistry for high-rate and long-life proton batteries. *Nat. Energy* 4:123–30
72. Giordani M, Berto M, Di Lauro M, Bortolotti CA, Zoli M, Biscarini F. 2017. Specific dopamine sensing based on short-term plasticity behavior of a whole organic artificial synapse. *ACS Sens.* 2:1756–60
73. Banerjee W. 2020. Challenges and applications of emerging nonvolatile memory devices. *Electronics* 9:1029
74. Qian C, Sun J, Kong L-A, Gou G, Yang J, et al. 2016. Artificial synapses based on in-plane gate organic electrochemical transistors. *ACS Appl. Mater. Interfaces* 8:26169–75
75. Gkoupidenis P, Schaefer N, Strakosas X, Fairfield JA, Malliaras GG. 2015. Synaptic plasticity functions in an organic electrochemical transistor. *Appl. Phys. Lett.* 107:263302
76. Berzina T, Smerieri A, Bernabò M, Pucci A, Ruggeri G, et al. 2009. Optimization of an organic memristor as an adaptive memory element. *J. Appl. Phys.* 105:124515
77. Zhou J, Anjum DH, Chen L, Xu X, Ventura IA, et al. 2014. The temperature-dependent microstructure of PEDOT/PSS films: insights from morphological, mechanical and electrical analyses. *J. Mater. Chem. C* 2:9903–10
78. Kim S-M, Kim C-H, Kim Y, Kim N, Lee W-J, et al. 2018. Influence of PEDOT:PSS crystallinity and composition on electrochemical transistor performance and long-term stability. *Nat. Commun.* 9:3858
79. Gumyusenge A, Luo X, Ke Z, Tran DT, Mei J. 2019. Polyimide-based high-temperature plastic electronics. *ACS Mater. Lett.* 1:154–57
80. Gumyusenge A, Tran DT, Luo X, Pitch GM, Zhao Y, et al. 2018. Semiconducting polymer blends that exhibit stable charge transport at high temperatures. *Science* 362:1131–34
81. Arnold C Jr. 1979. Stability of high-temperature polymers. *J. Polym. Sci. Macromol. Rev.* 14:265–378
82. Meine N, Benedito F, Rinaldi R. 2010. Thermal stability of ionic liquids assessed by potentiometric titration. *Green Chem.* 12:1711–14
83. Villanueva M, Coronas A, García J, Salgado J. 2013. Thermal stability of ionic liquids for their application as new absorbents. *Ind. Eng. Chem. Res.* 52:15718–27
84. Song E, Li J, Won SM, Bai W, Rogers JA. 2020. Materials for flexible bioelectronic systems as chronic neural interfaces. *Nat. Mater.* 19:590–603

85. Rogers J, Bao Z, Lee T-W. 2019. Wearable bioelectronics: opportunities for chemistry. *Acc. Chem. Res.* 52:521–22
86. Paulsen BD, Tybrandt K, Stavrinidou E, Rivnay J. 2020. Organic mixed ionic–electronic conductors. *Nat. Mater.* 19:13–26
87. van Doremaele ERW, Gkoupidenis P, van de Burgt Y. 2019. Towards organic neuromorphic devices for adaptive sensing and novel computing paradigms in bioelectronics. *J. Mater. Chem. C* 7:12754–60
88. Maya-Vetencourt JF, Ghezzi D, Antognazza MR, Colombo E, Mete M, et al. 2017. A fully organic retinal prosthesis restores vision in a rat model of degenerative blindness. *Nat. Mater.* 16:681–89
89. Maya-Vetencourt JF, Manfredi G, Mete M, Colombo E, Bramini M, et al. 2020. Subretinally injected semiconducting polymer nanoparticles rescue vision in a rat model of retinal dystrophy. *Nat. Nanotechnol.* 15:698–708
90. Dickey AS, Suminski A, Amit Y, Hatsopoulos NG. 2009. Single-unit stability using chronically implanted multielectrode arrays. *J. Neurophysiol.* 102:1331–39
91. Taunyazov T, Sng W, See HH, Lim B, Kuan J, Ansari FA, et al. 2020. Event-driven visual-tactile sensing and learning for robots. arXiv:2009.07083 [cs.RO]
92. Lee WW, Tan YJ, Yao H, Li S, See HH, et al. 2019. A neuro-inspired artificial peripheral nervous system for scalable electronic skins. *Sci. Robot.* 4:eaax2198
93. Li P, Anwar Ali HP, Cheng W, Yang J, Tee BCK. 2020. Bioinspired prosthetic interfaces. *Adv. Mater. Technol.* 5:1900856
94. Lee Y, Lee T-W. 2019. Organic synapses for neuromorphic electronics: from brain-inspired computing to sensorimotor nervetronics. *Acc. Chem. Res.* 52:964–74
95. Mikhaylov A, Pimashkin A, Pigareva Y, Gerasimova S, Gryaznov E, et al. 2020. Neurohybrid memristive CMOS-integrated systems for biosensors and neuroprosthetics. *Front. Neurosci.* 14:358
96. Tarabella G, D'Angelo P, Cifarelli A, Dimonte A, Romeo A, et al. 2015. A hybrid living/organic electrochemical transistor based on the *Physarum polycephalum* cell endowed with both sensing and memristive properties. *Chem. Sci.* 6:2859–68
97. Juzekaeva E, Nasretdinov A, Battistoni S, Berzina T, Iannotta S, et al. 2019. Coupling cortical neurons through electronic memristive synapse. *Adv. Mater. Technol.* 4:1800350
98. Gkoupidenis P, Koutsouras DA, Lonjaret T, Fairfield JA, Malliaras GG. 2016. Orientation selectivity in a multi-gated organic electrochemical transistor. *Sci. Rep.* 6:27007
99. Qian C, Kong L-A, Yang J, Gao Y, Sun J. 2017. Multi-gate organic neuron transistors for spatiotemporal information processing. *Appl. Phys. Lett.* 110:083302
100. Rivnay J, Inal S, Salleo A, Owens RM, Berggren M, Malliaras GG. 2018. Organic electrochemical transistors. *Nat. Rev. Mater.* 3:17086
101. Khodagholy D, Gelinas JN, Thesen T, Doyle W, Devinsky O, et al. 2015. NeuroGrid: recording action potentials from the surface of the brain. *Nat. Neurosci.* 18:310–15
102. Keene ST, Lubrano C, Kazemzadeh S, Melianas A, Tuchman Y, et al. 2020. A biohybrid synapse with neurotransmitter-mediated plasticity. *Nat. Mater.* 19:969–73
103. Iino Y, Sawada T, Yamaguchi K, Tajiri M, Ishii S, et al. 2020. Dopamine D2 receptors in discrimination learning and spine enlargement. *Nature* 579:555–60
104. Lee Y, Oh JY, Xu W, Kim O, Kim TR, et al. 2018. Stretchable organic optoelectronic sensorimotor synapse. *Sci. Adv.* 4:eaat7387
105. Kim Y, Chortos A, Xu W, Liu Y, Oh JY, et al. 2018. A bioinspired flexible organic artificial afferent nerve. *Science* 360:998–1003
106. Jörntell H, Bengtsson F, Geborek P, Spanne A, Terekhov AV, Hayward V. 2014. Segregation of tactile input features in neurons of the cuneate nucleus. *Neuron* 83:1444–52

Annual Review of Materials Research

Volume 51, 2021

Contents

Current Interest

Indexes

Errata

An online log of corrections to *Annual Review of Materials Research* articles may be found at http://www.annualreviews.org/errata/matsci